Journal of Materials Chemistry B

Accepted Manuscript

ROYAL SOCIETY OF CHEMISTRY

www.rsc.org/materialsB

Journal of Materials Chemistry B

COMMUNICATION

Fluorinated Smart Micelles as Enzyme-responsive Probes for ^{19}F-Magnetic Resonance

Received 00th January 20xx,
Accepted 00th January 20xx

DOI: 10.1039/x0xx00000x

www.rsc.org/

M. Buzhor,[a,b] L. Avram,[a] L. Frish,[a] Y. Cohen[a,b] and R. J. Amir*[,a,b]

Labeling of smart PEG-dendron hybrids with fluorinated groups transformed their assemblies into enzyme-responsive micellar probes for ^{19}F-magnetic resonance (MR). Two distinct labeling approches were used to study the ability of these smart hybrids to be turned OFF at the assembled micellar state and to turn ON their ^{19}F-MR signal upon enzymatic activation.

The development of biomedical imaging techniques including positron emission tomography (PET), computed tomography (CT), ultrasound, optical imaging and magnetic resonance imaging (MRI) has enabled acquisition of highly valuable anatomical information, which allows the diagnosis of diseases and monitoring of the progress of their medical treatment.[1] Among the various imaging tools, MRI serves as a highly important non-invasive tomographic imaging technique due to its high spatial resolution, deep tissue penetration and safety. In recent years major efforts have focused on the development of responsive MRI probes that posses sensitivity to the specific microenvironments of diseased tissues compared to healthy ones. These can be differences in pH values, over- or sub-expression of proteins or other molecular species, which if can be monitored, can provide important information about the status of the diseased tissues, organs and tumors.[2]

Potentially, the most appealing approach to design MRI probes is to design imaging probes that can response to pathologically relevant enzymes that are over-expressed in the target tissue. Pioneering work by Meade in the late 1990's reported a low molecular weight smart MRI contrast agent that was designed to respond to the enzyme β-galactosidase (an important marker for monitoring gene expression).[3] The enzymatic cleavage of a β-galactose moiety that was blocking the H_2O ligation site on a gadolinium atom, leaded to an irreversible 20% increase in relaxation rate. Since then, several similar approaches have been reported to modulate MRI contrast through the control of water access to a chelated paramagnetic center.[4] However, reliance on inner sphere hydration as the response mechanism of smart MRI probes, is not ideal due to potential anion interactions with the cleaved (more solvated/accessible) paramagnetic center, which has been identified to be a considerable interfering factor, particularly in vivo, where water-competing anions are abundant.[5]

An alternative approach for the design of stimuli-responsive magnetic resonance (MR) probes would be to use fluorinated stimuli-responsive amphiphilic block-copolymers as smart platforms that allow the supramolecular translation of the stimuli-induced disassembly into the turn-ON of the ^{19}F-MR signal. The motivation to use ^{19}F is that compared to ^{1}H-MRI, ^{19}F-MRI has almost no biological background due to the absence of fluorine in the body. Furthermore, ^{19}F has 100% natural abundance and its gyromagnetic ratio (40.06 MHz/T), which is second only to ^{1}H, makes it more sensitive for detection over other nuclei.[6] Stimuli-responsive polymers have gained increasing interest due to their potential applications ranging from drug delivery to tissue engineering.[7–9] In recent years smart polymers were further exploited to transform non-responsive fluorescent dyes into responsive dyes by utilizing the ability of these polymers to change their structure in response to stimuli, such as changes in pH,[10] temperature[11] and chemical analytes.[9] These structural changes were shown to alter the microenvironments of the dyes, which responded by spectral changes.[10]

For MR probes, the supramolecular translation mechanism may rely on the expected changes in spin-spin relaxation (T_2) when going from micellar or aggregated states into a monomeric non-assembled form. In the assembled form, the T_2 relaxation time should be extremely short and hence the fluorinated responsive block is expected to be in its OFF state and show almost no signal due to its extremely low mobility. Upon stimuli, the increase in hydrophilicity should result in increase in the mobility of the responsive fluorinated-block

[a] *Department of Organic Chemistry, School of Chemistry, Faculty of Exact Sciences, Tel-Aviv University, Tel-Aviv 69978, Israel.*
[b] *Tel Aviv University Center for Nanoscience and Nanotechnology, Tel-Aviv University, Tel-Aviv 69978, Israel.*
Email: amirroey@tau.ac.il. *Tel: +972 3 6408435.*
Electronic Supplementary Information (ESI) available: [Synthetic procedures, DLS data, spectral data and experimental parameters]. See DOI: 10.1039/x0xx00000x

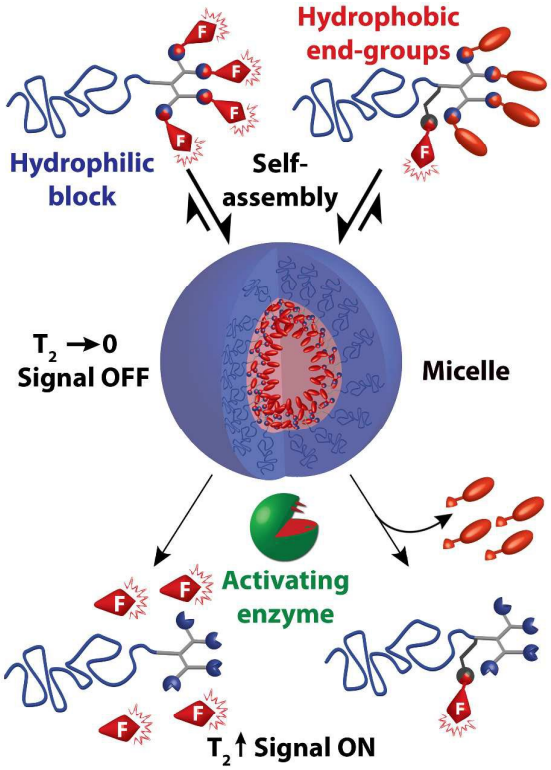

Figure 1: Illustration of the supramolecular translation mechanism for the two types of molecular architectures: cleavable fluorine-containing end-groups (on the left) and non-cleavable labelling of the polymer with fluorine containing probe (on the right). At the assembled state, aggregation of the hydrophobic fluorinated groups at the core of the micelles results in extremely short T_2 relaxation time, leading to an OFF state. Upon enzymatic activation the mobility of the fluorinated derivatives: fluorinated hydrophilic polymer or cleaved low molecular weight fluorine containing end-groups, increases and their magnetic resonance signal is turned ON.

and its T_2 relaxation time, leading to turning ON of the MR signal. This approach was recently demonstrated by Gao and Sherry,[14] which elegantly utilized fluorine containing pH responsive block copolymers in order to prepare ^{19}F-NMR/MRI nanoprobes that can be turned ON at different pH levels based on the pKa values of the pH-responsive amine moieties. More recently, Thayumanavan and coworkers reported the use of fluorine-containing groups that were linked through cleavable ester bonds to amphiphilic dendrons.[15] These fluorinated dendrons formed sub-micron assemblies that showed a broad peak in the absence of the esterase. The addition of the activating enzyme resulted in the formation of a new sharp peak at slightly higher chemical shift, due to the release of the low molecular weight fluorinated end-groups that were cleaved by the enzyme.

Recently we reported highly modular amphiphilic hybrids based on hydrophilic PEG block and a hydrophobic enzyme-responsive dendrons, which could assemble into smart micellar nanocarriers.[16,17] Labeling of these smart hybrids with non-cleavable fluorescent dyes turned them into a generic supramolecular platform for the translation of structural changes into fluorescent responses.[17,18] The translation mechanism was based on the unique spectral properties of the assembled micelles in comparison with the free labeling fluorescent dyes. Here we demonstrate that these smart hybrids can be easily transformed into enzyme-responsive ^{19}F-MR probes by simply replacing the dyes with fluorinated labeling moieties or end-groups. These probes are expected to turn ON their magnetic resonance signal upon enzymatic activation, as the fluorinated derivatives become more hydrophilic and their mobility and T_2 relaxation increase. Two orthogonal architectures bearing the fluorinated probe moieties, either as cleavable end-groups or as non-cleavable label between the PEG and dendron (Figure 1), were used in order to test the postulated translation mechanism. In both cases a significant change in T_2 relaxation can be expected, due to direct enzymatic cleavage of the fluorinated end-groups or increase in hydrophilicity and disassembly of the fluorinated hydrophilic hybrids.

Hybrids **1** and **2** (Scheme 1) were chosen as model compounds that can be activated by Porcine Liver Esterase (PLE).[19] 4-(Trifluoromethyl)phenylacetic acid was chosen as labeling group as it contains three equivalent fluorine atoms and a carboxylic acid that could be easily used for both the esterification and amidation based labeling steps. The two hybrids were synthesized directly on the PEG through accelerated dendritic growth approach[20] using amidation and thiol-yne[21,22] chemistries to build the dendrons. The synthesized hybrids and their fully hydrolyzed derivatives **1a**[17] and **2a** were obtained in high yields and characterized by ^{1}H-NMR, ^{13}C-NMR, ^{19}F-NMR, IR, GPC, HPLC and MALDI-MS) and the experimental data was found to be in good agreement with the theoretical one (see SI).

Characterization of the self-assembled micelles

The critical micelle concentrations (CMC) were determined using Nile red[23] and both hybrids were found to have CMC values at the low micro-molar range (2 +/- 1 μM and 4 +/- 1 μM for hybrids **1** and **2**, respectively, Figure S12). Dynamic light scattering (DLS) measurements showed diameters of 26 +/- 4 nm for hybrid **1** (Figure S13) and 16 +/- 3 nm for hybrid **2** (Figure S14), which fit micellar assemblies and are in good correlation with our previous results.[16–18] The translation of the supramolecular structural changes into MR spectral responses depend on the differences in the spin-spin T_2 relaxation times of the labeled polymers at the assembled and disassembled state, after their enzymatic activation. Hence, once the self-assembly of both hybrids into micelles was confirmed, we measured their T_1 and T_2 relaxation times and compared them to the values of synthetically obtained hydrophilic hybrids **1a** and **2a** (Table 1). We were encouraged to see that both hybrids showed significant increase in both T_1 and T_2 values going from the amphiphilic hybrids to the hydrophilic ones. It is important to note that greater change was observed for hybrid **1**. This can be rationalized by considering that in the case of hybrid **2** the fluorinated probe molecule remains attached to the hydrophilic polymer after the enzymatic activation and hence the mobility and T_2

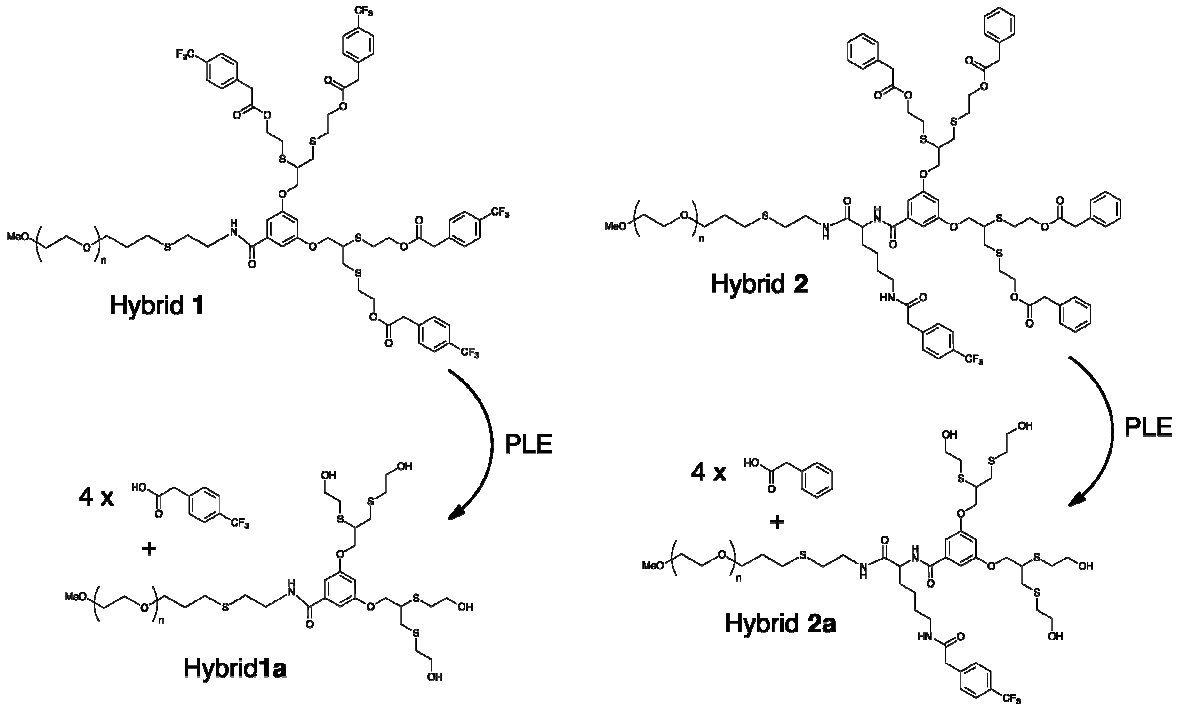

Scheme 1: Structures of hybrids **1** and **2** and their fully hydrolyzed hydrophilic derivatives, **1a** and **2a**, respectively.

increase but not to the same extent as for the small molecules that are released from hybrid **1**.

Structural and spectral responses

To study the structural and spectral responses of the micelles, we first studied their disassembly by DLS measurements, which showed a clear disappearance of the larger micellar structures and formation of smaller spices with diameters of around 4-7 nm (Figure S13 and S14), which fit well with the disassembly of the micelles into soluble hydrophilic hybrids. To get kinetic information on the disassembly process, we combined fluorescence spectroscopy, HPLC and ^{19}F-NMR. As the focus of this work is the MR response, we used equimolar concentrations of the fluorine atoms for both hybrids (160 μM and 640 μM for hybrids **1** and **2**, respectively) and the concentration of the enzyme was set to 1.1 μM. Fluorescence spectroscopy was used to study the release of encapsulated Nile red upon enzymatic activation as upon its release from the disassembling micelles into the aqueous environment its fluorescence decreases. The obtained spectra for both hybrids showed the expected decrease in the fluorescence of the released Nile red molecules in the presence of the enzyme (Figures S15 and S16) while no change was observed in the absence of the enzyme (Figures S17 and S18), further supporting the enzymatic-induced disassembly. Both the DLS and the fluorescence spectra gave clear indication that the micelles break down upon enzymatic activation to release their molecular cargo. However these techniques do not reveal the exact degree of activation. In order to obtain direct analysis of the polymeric components during the disassembly process we used HPLC to follow the enzymatic degradation. The HPLC data of both hybrids showed direct enzymatic transformation of hybrids **1** and **2** into the corresponding hydrophilic hybrids **1a** and **2a**, respectively (Figures 2a and 2b)**.** Next, we studied the enzymatic activation by using ^{19}F-NMR and correlated it with the fluorescence and HPLC data. The acquisition parameters were set so ensure that the peaks of the assembled states and the cleaved end-groups (for hybrid **1**) or the labeled hydrophilic hybrid **2a** were visible and could be integrated (sodium fluoride was used as internal reference and its chemical shift was set to zero). Kinetic ^{19}F-NMR measurements clearly showed the disappearance of the peaks corresponding to the assembled states and appearances of new peaks that result from the cleaved fluorinated end-groups (for hybrid **1**) or the formation of labeled hydrophilic hybrid **2a** (Figures 2c and 2d). Excellent correlations were observed when plotting the HPLC and ^{19}F-NMR peaks areas for both hybrids as a function of time and these results correlated well with the fluorescence data for Nile red, which is indicative of

Table 1: ^{19}F-NMR relaxation times T_1 and T_2 of hybrids **1** and **2** before and after enzymatic activation. Hybrids **1a** and **2a** in the presence of the enzyme were used as control. (9.4T, 376 MHz, TE = 80 ms)

Hybrid	1	1+PLE	1a+PLE	2	2+PLE	2a+PLE
T_1 (ms)	910 +/- 30	2040 +/- 60	1920 +/- 90	860 +/- 90	1090 +/- 50	1090 +/- 30
T_2 (ms)	9 +/- 1	1260 +/- 6	1390 +/- 100	16 +/- 3	320 +/- 40	450 +/- 15

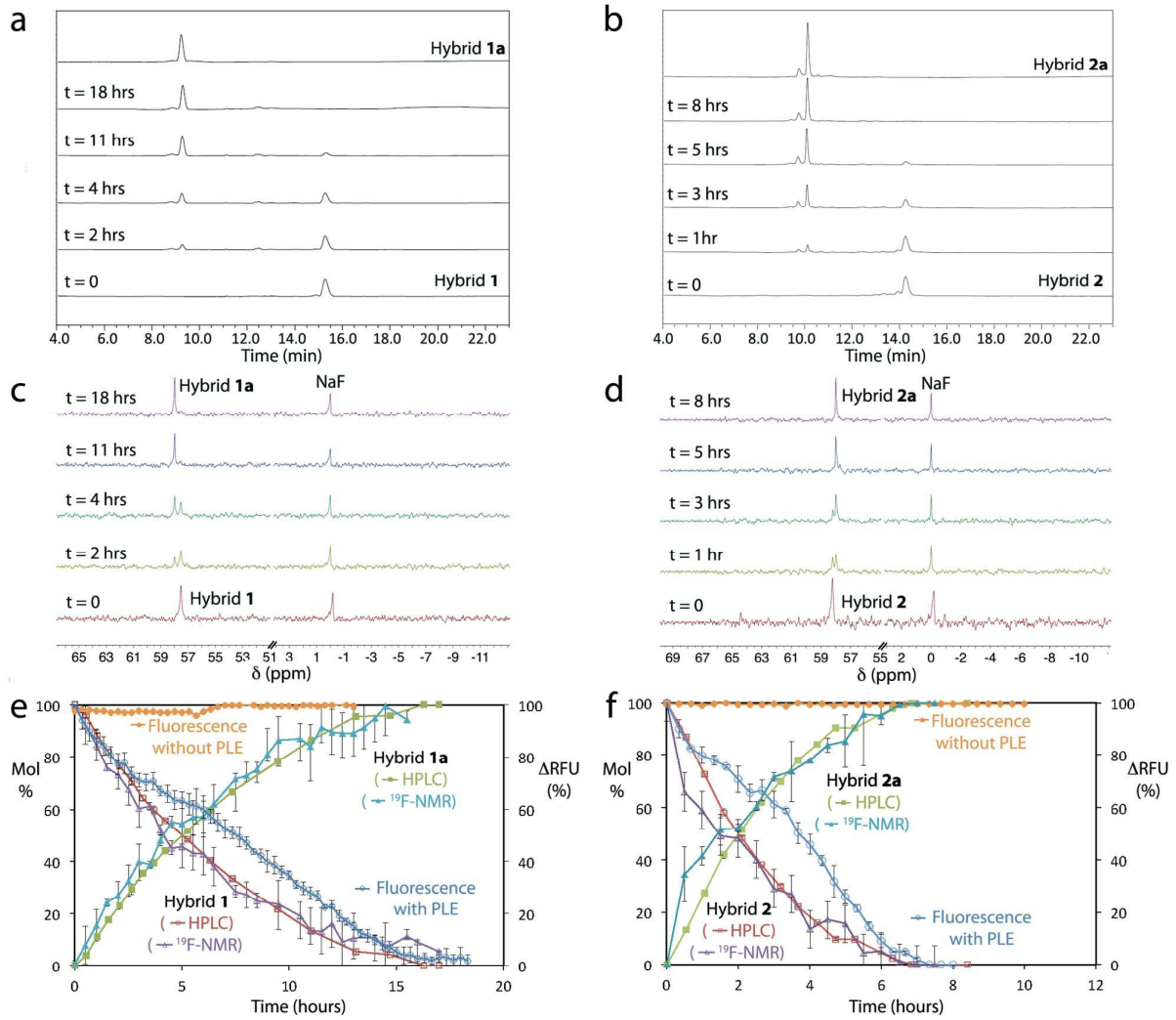

Figure 2: Overlay of HPLC chromatograms (a and b), ^{19}F-NMR spectra (c and d) and kinetic data (HPLC, ^{19}F-NMR and fluorescence) for the enzymatic-induced activation of hybrids **1** (e) and **2** (f).

the presence of micelles (Figures 2e and 2f). Notably, although the concentration of hybrid **2** was four times higher, its enzymatic activation was completed in nearly third of the time that was observed for hybrid **1**. This decrease in enzymatic activity is most likely due to poorer matching between the enzyme and the trifluoromethyl containing substrates in comparison with the non-substituted substrate.

After the disassembly of both types of micelles upon enzymatic activation was confirmed, we set to explore their ability to show clear OFF/ON states. To do so, we used a spin-echo ^{19}F-NMR sequence (see SI) to measure the spectra before the addition of the enzyme and after the disassembly was completed (Figure 3). This sequence allows us to utilize the significant differences in T_2 relaxation times between the assembled and disassembled states. We were encouraged to see that the obtained spectra didn't show any signal for the assembled states of either hybrid **1** or **2**, while the reference peak of NaF was clearly observed in both spectra, indicating

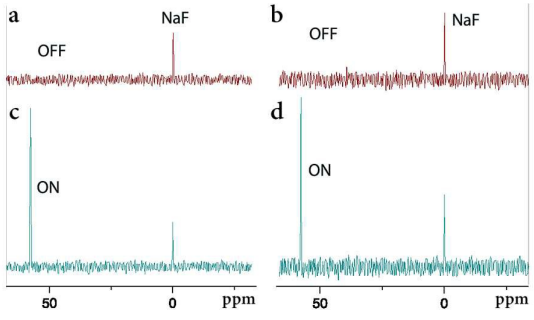

Figure 3: ^{19}F-NMR spectra obtained by spin-echo sequence (9.4T, 376 MHz, TE = 80 ms) showing the micellar OFF states and ON states after the disassembly of hybrids **1** (a – OFF; c – ON) and **2** (b – OFF; d - ON).

the OFF state of the assembled micelles (Figures 3a and 3c). We were then delighted when the spectra of the disassembled hybrids clearly showed the peaks correlating with the end-

groups that were cleaved from hybrid **1** or with hydrophilic hybrid **2a**, demonstrating the enzymatic-turn ON of the ^{19}F-MR signals (Figures 3b and 3d).

To further demonstrate that this supramolecular approach could be applied also for ^{19}F-MRI, we carried out very preliminary imaging experiments with hybrid **1**, which although it had slower activation rate, its increase in T_2 relaxation time when going from OFF to ON state ($T_{2(ON)}/T_{2(OFF)}$ = 140) was significantly higher in comparison with hybrid **2** ($T_{2(ON)}/T_{2(OFF)}$ = 20). A solution of Hybrid **1** in the absence of the enzyme was placed in a 5mm NMR tube, which was placed in another 8mm NMR tube containing the hybrid and the enzyme (Figure 4a). While the ^{1}H-MRI image showed no difference between the inner tube and the outer one, a clear difference was observed in the spin-echo ^{19}F-MR image. A bright signal was obtained only for the enzyme containing outer tube with an ON/OFF ratio of 3.3, which could be improved to 5.1 using echo-planar imaging (EPI), which gave better contrast but also showed some artifacts in regard to the contour of the tubes (see SI).

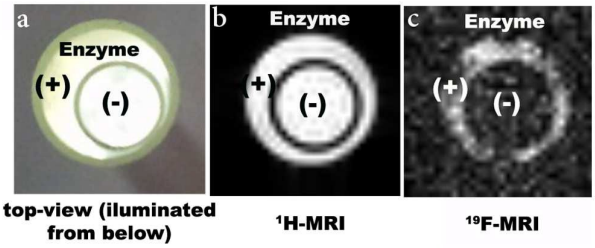

Figure 4: A photo of a 5 mm NMR tube with the micelles of hybrid **1** inside an outer 8 mm tube containing enzymatically-activated micelles (a). Spin-echo ^{1}H-MRI (b) and spin-echo ^{19}F-MRI (c) images (14.1T, 600 MHz (^{1}H)/564 MHz (^{19}F), TE = 8 ms, TR = 700 ms).

Conclusions

In summary, we report the rational design of highly modular enzyme-responsive MR probes for ^{19}F-MR based on smart fluorinated amphiphilic hybrids. Two diverse molecular approaches were explored by using either fluorinated cleavable end-groups or non-cleavable labeling of the polymeric backbone. Both molecular designs were studied by combination of DLS, Fluorescence spectroscopy, HPLC and NMR and were shown to be OFF at the assembled micellar state. Upon enzymatic activation and cleavage of the hydrophobic end-groups, both types of micelles disassembled and the MR signals were turned ON. In addition to the turn-ON of ^{19}F-NMR signals, we demonstrate the feasibility of the reported hybrids to serve as ^{19}F-MRI probes by carrying out preliminary MRI measurements with one of the reported structures. The comparison of the two architectures clearly showed that while fluorinated reporting end-groups allow the introduction of more fluorine atoms and hence stronger signals, the presence of fluorine atoms might also interfere with the enzymatic activity, leading to slower kinetics. The obtained results clearly prove the great potential of enzyme-responsive smart polymers to serve as an innovative and modular platform for the rational design of responsive MR probes. The next steps in the translation of this molecular approach towards biomedical application will be to study the biocompatibility of such micelles and their stability in biological media, such as cell medium and serum. Further biological studies and the introduction of additional activating enzymes and fluorine-containing probes are currently under investigation.

Acknowledgments

R.J. Amir thanks the Israel Science Foundation (grants No. 966/14 and 2221/14) for funding. We thank Natalya (Tesh) Weber for her help with preparing the graphics and Dr. Amir Goldbourt (TAU) for his helpful advice.

Notes and references

1 R. Weissleder, *Nat. Rev. Cancer*, 2002, **2**, 11–8.
2 G.-L. Davies, I. Kramberger and J. J. Davis, *Chem. Commun. (Camb).*, 2013, **49**, 9704–21.
3 A. Y. Louie, M. M. Hüber, E. T. Ahrens, U. Rothbächer, R. Moats, R. E. Jacobs, S. E. Fraser and T. J. Meade, *Nat. Biotechnol.*, 2000, **18**, 321–5.
4 R. Napolitano, G. Pariani, F. Fedeli, Z. Baranyai, M. Aswendt, S. Aime and E. Gianolio, *J. Med. Chem.*, 2013, **56**, 2466–77.
5 J. A. Duimstra, F. J. Femia and T. J. Meade, *J. Am. Chem. Soc.*, 2005, **127**, 12847–5
6 I. Tirotta, A. Mastropietro, C. Cordiglieri, L. Gazzera, F. Baggi, G. Baselli, M. G. Bruzzone, I. Zucca, G. Cavallo, G. Terraneo, F. Baldelli Bombelli, P. Metrangolo and G. Resnati, *J. Am. Chem. Soc.*, 2014, **136**, 8524–7.
7 J. Hu, G. Zhang and S. Liu, *Chem. Soc. Rev.*, 2012, **41**, 5933.
8 D. Roy, J. N. Cambre and B. S. Sumerlin, *Prog. Polym. Sci.*, 2010, **35**, 278–301.
9 A. P. Blum, J. K. Kammeyer, A. M. Rush, C. E. Callmann, M. E. Hahn and N. C. Gianneschi, *J. Am. Chem. Soc.*, 2015, **137**, 2140–2154.
10 K. Zhou, H. Liu, S. Zhang, X. Huang, Y. Wang, G. Huang, B. D. Sumer and J. Gao, *J. Am. Chem. Soc.*, 2012, **134**, 7803–11.
11 J. Qiao, L. Qi, Y. Shen, L. Zhao, C. Qi, D. Shangguan, L. Mao and Y. Chen, *J. Mater. Chem.*, 2012, **22**, 11543–11549.
12 Y. Jiang, X. Hu, J. Hu, H. Liu, H. Zhong and S. Liu, *Macromolecules*, 2011, **44**, 8780–8790.
13 C. Li and S. Liu, *Chem. Commun. (Camb).*, 2012, **48**, 3262–78.
14 X. Huang, G. Huang, S. Zhang, K. Sagiyama, O. Togao, X. Ma, Y. Wang, Y. Li, T. C. Soesbe, B. D. Sumer, M. Takahashi, a. D. Sherry and J. Gao, *Angew. Chemie - Int. Ed.*, 2013, **52**, 8074–8078.
15 H. Wang, K. R. Raghupathi, J. Zhuang and S. Thayumanavan, *ACS Macro Lett.*, 2015, **4**, 422–425.
16 A. J. Harnoy, I. Rosenbaum, E. Tirosh, Y. Ebenstein, R. Shaharabani, R. Beck and R. J. Amir, *J. Am. Chem. Soc.*, 2014, **136**, 7531–4.
17 I. Rosenbaum, A. J. Harnoy, E. Tirosh, M. Buzhor, M. Segal, L. Frid, R. Shaharabani, R. Avinery, R. Beck and R. J. Amir, *J. Am. Chem. Soc.*, 2015, **137**, 2276–2284.
18 M. Buzhor, A. J. Harnoy, E. Tirosh, A. Barak, T. Schwartz and R. J. Amir, *Chem. - A Eur. J.*, 2015, **21**, 15633–15638.
19 F. Wang, A. Klaikherd and S. Thayumanavan, *J. Am. Chem. Soc.*, 2011, **133**, 13496–13503.
20 M. V. Walter and M. Malkoch, *Chem. Soc. Rev.*, 2012, **41**, 4593.

21 R. Hoogenboom, *Angew. Chemie - Int. Ed.*, 2010, **49**, 3415–3417.
22 A. B. Lowe, *Polymer (Guildf).*, 2014, **55**, 5517–5549.
23 C. M. A. Leenders, L. Albertazzi, T. Mes, M. M. E. Koenigs, A. R. A. Palmans and E. W. Meijer, *Chem. Commun. (Camb).*, 2013, **49**, 1963–5.

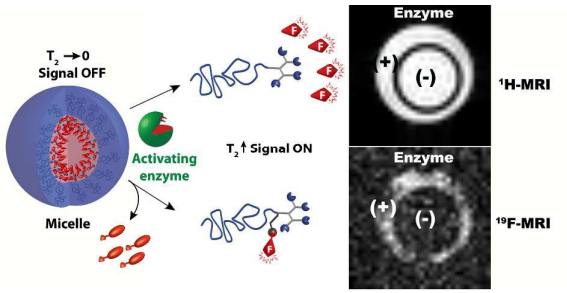

Labeling smart PEG-dendron hybrids with fluorine-containing groups transfrom their micelles into enzyme-responsive probes for ^{19}F-Magnetic Resonance.